

Self-Guided Belief Propagation – A Homotopy Continuation Method

Christian Knoll, *Student Member, IEEE*, Florian Kulmer, and Franz Pernkopf, *Senior Member, IEEE*

Abstract—We propose self-guided belief propagation (SBP) that modifies belief propagation (BP) by incorporating the pairwise potentials only gradually. This homotopy continuation method converges to a unique solution and increases the accuracy without increasing the computational burden. We apply SBP to grid graphs, complete graphs, and random graphs with random Ising potentials and show that: (i) SBP is superior in terms of accuracy whenever BP converges, and (ii) SBP obtains a unique, stable, and accurate solution whenever BP does not converge. We further provide a formal analysis to demonstrate that SBP obtains the global optimum of the Bethe approximation for attractive models with unidirectional fields.

Index Terms—Graphical models, belief propagation, probabilistic inference, sum-product algorithm, partition function, inference algorithms.

1 INTRODUCTION

COMPUTING the marginal distribution and evaluating the partition function are two fundamental problems of probabilistic graphical models. Both problems are NP-hard to solve [4], which substantiates the need for efficient approximation methods.

Belief propagation (BP) provides an efficient way to approximate the marginal distribution and has a long success story in many applications, including computer vision, speech processing, social network analysis, and error correcting codes [13], [17], [25]. It is, however, still an open problem to obtain a rigorous understanding of the limitations of BP for general graphs, where BP may fail to converge because: (i) multiple solutions exist, and it depends on implementation details to which one BP converges; (ii) one or all fixed points are unstable and messages oscillate far away from any fixed point [12], [23], [37]. These limitations motivate the search for modifications of BP that overcome these issues in order to increase the accuracy and enhance the convergence properties.

One way to provide convergence-guarantees is to consider an equivalent optimization problem that minimizes the Bethe free energy \mathcal{F}_B . This, however, comes at the cost of an increased runtime complexity; polynomial-time algorithms only exist for restricted classes of problems and even approximating the global minimum might be problematic for graphical models with arbitrary potentials [3], [28], [39]. Hence, the pursuit for methods that approximate the marginals with both runtime- and convergence-guarantees is still ongoing.

In this work, we present self-guided belief propagation (SBP) that aims to fill this gap. The observation that strong pairwise potentials reduce accuracy and deteriorate the convergence properties [15] inspired us to construct a homotopy; i.e., we first consider only local potentials (where BP is exact) and subsequently modify the model by increasing the pairwise potentials to the desired values. SBP thus solves a deterministic sequence of models that

iteratively refines the Bethe approximation towards an accurate solution that is uniquely defined by the initial model.

We evaluate SBP for grid-graphs, complete graphs, and random graphs with Ising potentials and, compared to BP, we observe superior performance in terms of accuracy; in fact SBP achieves more accurate results than Gibbs sampling in a fraction of runtime. We theoretically demonstrate optimality of the selected fixed point for *attractive*¹ models with unidirectional local potentials. Additionally SBP enhances the convergence properties and excels for *general* models where SBP provides accurate results despite the non-convergence of BP. We further expect that the ease of use lowers the hurdle for practical applications.

The paper is structured as follows: Section 2 provides some background on probabilistic graphical models, belief propagation, and methods that minimize the free energy. Our proposed algorithm is presented in Section 3 and important properties are presented subsequently. We evaluate SBP and discuss empirical observations in Section 4 and provide a more formal analysis in Section 5. Finally we conclude the paper in Section 7.

2 BACKGROUND

In this section, we briefly introduce probabilistic graphical models and specify the models considered in this work. We further introduce the BP algorithm and its connection to the Bethe approximation.

2.1 Probabilistic Graphical Models

Let us consider an undirected graph $\mathcal{G} = (\mathbf{X}, \mathbf{E})$, where $\mathbf{X} = \{X_1, \dots, X_N\}$ is the set of nodes, and \mathbf{E} is the set of undirected edges. Then, two nodes X_i and X_j are joined by an edge if $e_{ij} \in \mathbf{E}$. We denote the set of neighbors X_i by $\partial(X_i) = \{X_j \in \mathbf{X} : e_{ij} \in \mathbf{E}\}$.

Let us define a probabilistic graphical model $\mathcal{U} = (\mathcal{G}, \Psi)$ where $\Psi = \{\Phi_1, \dots, \Phi_K\}$ is the set of all K potentials and \mathbf{X}

1. An attractive model is a probabilistic graphical model where all pairwise interactions are specified by positive couplings; a general model contains pairwise interactions with negative couplings as well (cf. Sec 2.2).

• Christian Knoll (christian.knoll.c@ieee.org), Florian Kulmer (florian_kulmer@gmx.at), and Franz Pernkopf (pernkopf@tugraz.at) are with the Signal Processing and Speech Communication Laboratory, Graz University of Technology.

is the set of random variables. In this work we focus on pairwise models, i.e., all potentials consist of two variables at most, so that the joint distribution factorizes according to

$$P_{\mathbf{X}}(\mathbf{x}) = \frac{1}{\mathcal{Z}} \prod_{e_{ij} \in \mathbf{E}} \Phi_{X_i, X_j}(x_i, x_j) \prod_{i=1}^N \Phi_{X_i}(x_i), \quad (1)$$

where each edge is only considered once, i.e., $e_{ij} = e_{ji}$.

We consider the following two problems: (i) evaluation of the partition function \mathcal{Z} , which is the normalization function of the joint distribution. (ii) obtaining the marginal distribution

$$P_{\mathbf{X}_m} = \sum_{x_i: X_i \in \{\mathbf{X} \setminus \mathbf{X}_m\}} P_{\mathbf{X}}(x_i). \quad (2)$$

where $\mathbf{X}_m \subset \mathbf{X}$ may be any set of RVs. Evaluating the partition function is equivalent to minimizing the free energy where $\min \mathcal{F} = \mathcal{F}^* = -\ln \mathcal{Z}$ [43]. Note that both problems considered are in fact equivalent as \mathcal{F} obtains its minimum precisely for the marginal distribution, but are intractable in general [4].

Relaxing the problem by only approximating the marginal distribution and the partition function admits an elegant iterative algorithm. This method was discovered multiple times in different fields and is known as belief propagation (BP) in computer science, the sum-product algorithm in information theory, and the cavity- or the Bethe-method in physics (cf. Sec. 2.3); we refer the reader to [18], [22] for a good overview. The observation that fixed points of BP are in a one-to-one correspondence with stationary points of the Bethe free energy (cf. [43]) paved the way for a better understanding and alternative approaches that minimize the Bethe free energy directly (cf. Sec. 2.4).

2.2 MODEL SPECIFICATION

In this work we focus on Ising models, i.e., binary pairwise models where every random variable X_i takes values from $\mathbb{S} = \{-1, +1\}$. It is often more convenient to work with the mean (or magnetization)

$$m_i = \mathbb{E}(X_i) = P_{X_i}(X_i = 1) - P_{X_i}(X_i = -1) \quad (3)$$

and the correlation

$$\chi_{ij} = \mathbb{E}(X_i, X_j), \quad (4)$$

instead of considering the singleton marginals $P_{X_i}(x_i)$ and the pairwise marginals $P_{X_i, X_j}(x_i, x_j)$ explicitly. Let us define couplings $J_{ij} \in \mathbb{R}$ that are assigned to each edge $e_{ij} \in \mathbf{E}$ and local fields $\theta_i \in \mathbb{R}$ that act on each variable $X_i \in \mathbf{X}$. These parameters define the pairwise potentials $\Phi_{X_i, X_j}(x_i, x_j) = \exp(J_{ij}x_i x_j)$ and the local potentials $\Phi_{X_i}(x_i) = \exp(\theta_i x_i)$. The corresponding joint distribution from (5) is consequently given by

$$P_{\mathbf{X}}(\mathbf{x}) = \frac{1}{\mathcal{Z}} \exp\left(\sum_{e_{ij} \in \mathbf{E}} J_{ij} x_i x_j + \sum_{i=1}^N \theta_i x_i\right). \quad (5)$$

We distinguish two different types of interactions between random variables: if J_{ij} is negative then the edge e_{ij} is *repulsive*; if J_{ij} is positive then the edge e_{ij} is *attractive*. We call a model \mathcal{U} *attractive* if it contains only attractive edges,² and refer to it as *general* model otherwise.

2. Note that attractive models are also known as ferromagnetic models [22] or log-supermodular models [27].

2.3 BELIEF PROPAGATION (BP)

BP approximates the marginals by recursively exchanging messages between random variables. The messages from X_i to X_j at iteration $n+1$ are updated according to (6) and are normalized so that $\sum_{x_j \in \mathbb{S}} \mu_{ij}^n(x_j) = 1$.

$$\mu_{ij}^{n+1}(x_j) \propto \sum_{x_i \in \mathbb{S}} \Phi_{X_i, X_j}(x_i, x_j) \Phi_{X_i}(x_i) \prod_{X_k \in \{\partial(X_i) \setminus X_j\}} \mu_{ki}^n(x_i) \quad (6)$$

Let $\underline{\mu}^n = \{\mu_{ij}^n(x_j) : e_{ij} \in \mathbf{E}, x_j \in \mathbb{S}\}$ be the set of all messages at iteration n and let the mapping induced by (6) be denoted as

$$\underline{\mu}^{n+1} = \mathcal{BP}(\underline{\mu}^n). \quad (7)$$

If all successive messages remain unchanged, i.e., $\underline{\mu}^{n+1} = \underline{\mu}^n$, then BP is converged to a *fixed point* $\underline{\mu}^\circ$. We further write

$$\underline{\mu}^\circ = \mathcal{BP}^\circ(\underline{\mu}^\circ), \quad (8)$$

where \mathcal{BP}° performs BP until convergence. The singleton marginals P_{X_i} and pairwise marginals P_{X_i, X_j} are subsequently approximated by

$$\tilde{P}_{X_i}(x_i) = \frac{1}{Z_i} \Phi_{X_i}(x_i) \prod_{X_k \in \partial(X_i)} \mu_{ki}^\circ(x_i), \quad (9)$$

$$\tilde{P}_{X_i, X_j}(x_i, x_j) = \frac{1}{Z_{ij}} \Phi_{X_i}(x_i) \Phi_{X_j}(x_j) \Phi_{X_i, X_j}(x_i, x_j) \cdot \prod_{X_k \in \{\partial(X_i) \setminus X_j\}} \mu_{ki}^\circ(x_i) \cdot \prod_{X_l \in \{\partial(X_j) \setminus X_i\}} \mu_{lj}^\circ(x_j), \quad (10)$$

where $Z_i, Z_{ij} \in \mathbb{R}_+^*$ guarantee that all probabilities sum to one. These approximations further constitutes the pseudomarginals

$$\tilde{P}_{\mathbf{X}_B} := \{\tilde{P}_{X_i}, \tilde{P}_{X_i, X_j} : X_i \in \mathbf{X}, e_{ij} \in \mathbf{E}\}. \quad (11)$$

The performance of BP does not only depend on \mathcal{G} [37] but on the potentials Ψ as well [14], [23]. On Ising models BP converges to a unique stable fixed point if the couplings J_{ij} are weak (relative to θ_i). For attractive models with strong couplings multiple solutions exist and BP converges to one of them. For general models that contain strong couplings multiple solutions may exist and BP does not converge (even if the solution is unique) [15], [23]. Note that these differences in behavior coincide with different phases in statistical mechanics (cf. [22], [33], [45]).

If BP fails to converge and the messages oscillate, one can try to achieve convergence by either changing the update-rule [6], [16], [32], or by replacing the messages with a convex combination of the last messages [24]. The latter method is known as damping (BP_D) where a damping parameter $\epsilon \in [0, 1)$ specifies the new update rule

$$\begin{aligned} \underline{\mu}^{n+1} &= \mathcal{BP}_D(\underline{\mu}^n), \\ &= (1 - \epsilon)\mathcal{BP}(\underline{\mu}^n) + \epsilon\underline{\mu}^n. \end{aligned} \quad (12)$$

2.4 THE BETHE APPROXIMATION & RELATED WORK

The Bethe free energy $\mathcal{F}_B(\tilde{P}_{\mathbf{X}_B}) := E_B(\tilde{P}_{\mathbf{X}_B}) - S_B(\tilde{P}_{\mathbf{X}_B})$ is obtained by only considering the pseudomarginals (cf. (11)) where the energy $E_B(\tilde{P}_{\mathbf{X}_B})$ and the entropy $S_B(\tilde{P}_{\mathbf{X}_B})$ are defined by

$$E_B(\tilde{P}_{\mathbf{X}_B}) := -\sum_{\mathbf{x}_m: \mathbf{X}_m \in \mathbf{X}_B} \tilde{P}_{\mathbf{X}_m}(\mathbf{x}_m) \cdot \ln \Phi_{\mathbf{X}_m}(\mathbf{x}_m), \quad (13)$$

$$S_B(\tilde{P}_{\mathbf{X}_B}) := -\sum_{\mathbf{x}_m: \mathbf{X}_m \in \mathbf{X}_B} \tilde{P}_{\mathbf{X}_m}(\mathbf{x}_m) \cdot \ln \tilde{P}_{\mathbf{X}_m}(\mathbf{x}_m). \quad (14)$$

More specifically the Bethe free energy is given by

$$\begin{aligned} \mathcal{F}_B(\tilde{P}_{\mathbf{X}_B}) &= \sum_{e_{ij} \in \mathbf{E}} \sum_{x_i, x_j} \tilde{P}_{X_i, X_j}(x_i, x_j) \ln \frac{\tilde{P}_{X_i, X_j}(x_i, x_j)}{\Phi_{X_i, X_j}(x_i, x_j)} \\ &\quad - \sum_{X_i} \sum_{x_i} \tilde{P}_{X_i}(x_i) \ln \Phi_{X_i}(x_i) \\ &\quad - \sum_{X_i} (|\partial(X_i)| - 1) \sum_{x_i} \tilde{P}_{X_i}(x_i) \ln \tilde{P}_{X_i}(x_i). \end{aligned} \quad (15)$$

Note that BP is equivalent to minimizing \mathcal{F}_B over the local polytope $\mathcal{L} = \{\tilde{P}_{\mathbf{X}_B} : \sum \tilde{P}_{X_i} = 1, \sum_{X_j} \tilde{P}_{X_i, X_j} = \tilde{P}_{X_i}\}$, i.e., $\min_{\mathcal{L}}(\mathcal{F}_B) = \mathcal{F}_B^* = \mathcal{F}_B(\tilde{P}_{\mathbf{X}_B}^*)$ (cf. [10], [35, pp.77]), where the global minimum is denoted by \mathcal{F}_B^* . All (local) stationary points are further denoted by \mathcal{F}_B° and relate to the fixed points of BP and the associated pseudomarginals $\tilde{P}_{\mathbf{X}_B}^\circ$ by

$$\mathcal{F}_B^\circ = \mathcal{F}_B(\tilde{P}_{\mathbf{X}_B}^\circ), \quad (16)$$

where every stable fixed point $\tilde{P}_{\mathbf{X}_B}^\circ$ corresponds to a local minimum \mathcal{F}_B° ; the converse, however, need not be the case, i.e., not every local minimum of \mathcal{F}_B corresponds to a stable fixed point [36].

This correspondence between BP and \mathcal{F}_B led to a better understanding of BP and inspired plenty methods that minimize \mathcal{F}_B directly [41], [44]. The minimization, however, is still highly non-trivial and requires good approximation methods in practice. Strong pairwise potentials reduce the accuracy of the Bethe approximation and are responsible for its non-convexity [14]. One can therefore correct the entropy term (14) by accounting for the strong potentials; this admits convex relaxations that provide provable convergent message passing algorithms [7], [9], [20], [21], [34]. There is, however, a trade-off between convergence-properties and accuracy in general and the Bethe approximation often provides accurate results, if it can be minimized, and outperforms convex free energy approximations [21], [39]. Thus, it is a relevant problem to directly approximate \mathcal{F}_B in a way that allows for efficient minimization. Polynomial runtime algorithms exist that approximate \mathcal{F}_B for restricted models: these include sparsity constraints [28] or require *attractive* models [39]. If both properties are fulfilled, i.e., for locally tree-like attractive models the Bethe approximation is exact and can be optimized efficiently [5]. Note that \mathcal{F}_B provides an upper bound on \mathcal{F} for attractive models [27], [42].

We aim to efficiently approximate \mathcal{F}_B similar as in [39]: their approximation can be made ϵ -accurate; this, however, comes at the cost of giving up runtime guarantees for general models. Our work, on the contrary, provides an approximation in constant runtime (cf. Theorem 3 in Sec. 5); the approximation error, however, can not be made arbitrarily small for general models. Both methods overcome their respective disadvantages when restricting the models; i.e., both methods do efficiently minimize the Bethe approximation for attractive models.

3 SELF-GUIDED BELIEF PROPAGATION (SBP)

We start by an intuitive justification of the proposed method and subsequently introduce SBP in detail. We further present practical considerations and pseudocode of SBP. We provide a formal treatment of the properties of SBP in Sec. 5.

The current understanding of BP is that strong (pairwise) potentials negatively influence BP. The overall number of iterations can be reduced by incorporating the potentials slowly [2]. However, inspired by the recent observation that strong local potentials increase accuracy and lead to better convergence properties [15], we rather aim to only reduce the influence of the pairwise potentials that negatively influence BP. It is indeed worth considering whether an accurate fixed point emerges if we start from a simple model with independent random variables and slowly increase the potentials' strength [11]. SBP achieves this by homotopy continuation, i.e., it solves the simple problem first and – by repetitive application of BP, keeps track of the fixed point as the interaction strength is increased by a scaling term. We present pseudocode of the algorithm in Sec. 3.2.

More formally SBP considers an increasing length- M sequence $\{\zeta_m\}$ where $m = 1, \dots, M$ such that $\zeta_m < \zeta_{m+1}$ and $\zeta_m \in [0, 1]$ with $\zeta_1 = 0$ and $\zeta_M = 1$. This further indexes a sequence of probabilistic graphical models $\{\mathcal{U}_m\}$ that converges to the model of interest $\mathcal{U}_M = \mathcal{U}$. We further denote the fixed points of BP for \mathcal{U}_m by $\underline{\mu}_{[m]}^\circ$. Every probabilistic graphical model has a set of potentials $\Psi_{[m]} = \{\Phi_{X_i, X_j}(x_i, x_j)_{[m]}, \Phi_{X_i}(x_i)_{[m]}\}$ associated, where $\Phi_{X_i}(x_i)_{[m]} = \Phi_{X_i}(x_i)$ and the pairwise potentials at index m are exponentially scaled by

$$\begin{aligned} \Phi_{X_i, X_j}(x_i, x_j)_{[m]} &= \exp(J_{ij} \zeta_m x_i x_j) \\ &= \Phi_{X_i, X_j}(x_i, x_j)^{\zeta_m}. \end{aligned} \quad (17)$$

The initialization determines the performance of BP if multiple fixed points exist; SBP always provides a favorable initialization by the preceding fixed point and performs the composite function

$$\underline{\mu}_{[M]}^\circ = \mathcal{BP}_{[M]}^\circ \left(\mathcal{BP}_{[M-1]}^\circ \left(\dots \mathcal{BP}_{[1]}^\circ \left(\underline{\mu}_{[1]}^0 \right) \right) \right). \quad (18)$$

This may lead to problems if the fixed point becomes unstable for some value $m < M$. If the messages start to oscillate and BP does not converge within a pre-specified number of iterations it cannot be used to keep track of the fixed point. Instead, SBP provides the last stable fixed point in that case, i.e., $\underline{\mu}_{[M]}^\circ = \mathcal{BP}_{[m-1]}^\circ \left(\dots \mathcal{BP}_{[1]}^\circ \left(\underline{\mu}_{[1]}^0 \right) \right)$.

In other words SBP is an iterative algorithm that either provides a stationary point \mathcal{F}_B° , or an approximation thereof, if \mathcal{F}_B° is not stable with respect to BP. First, SBP relaxes the problem until all random variables are independent and the Bethe approximation is exact. Then, the problem is deformed into the original one by increasing ζ from zero to one. Consequently, \mathcal{F}_B is deformed such that the stationary point \mathcal{F}_B° emerges as a well-behaved path (cf. Prop. 1 in Sec. 5). SBP keeps track of this solution with BP constantly correcting the stationary point.

We illustrate how SBP keeps track of a fixed point in Fig. 1 for a problem where BP does not converge. Initially SBP obtains the pseudomarginals for $\zeta = 0$ by running BP on the simple model. Then, SBP estimates the pseudomarginals of the desired problem by successively increasing ζ and running BP. Indeed, a smooth solution path emerges and SBP is capable of tracking it. Note that the fixed point becomes unstable for $\zeta > 0.7$; SBP stops and provides the last stable solution as an approximation. Note that the approximated marginals are already close to the exact ones in this example; experiments show that this is often the case (cf. Sec. 4).

3.1 Practical considerations

In practice the runtime of SBP is influenced by the difference between two successive fixed points $\underline{\mu}_{[m]}^\circ$ and $\underline{\mu}_{[m-1]}^\circ$ – the

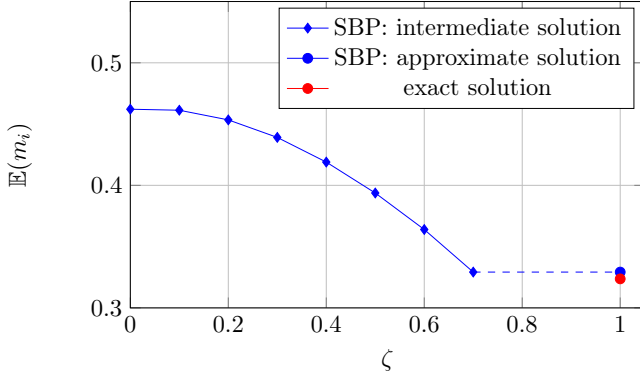


Fig. 1: Illustrative example: SBP proceeds along the smooth solution path and obtains accurate marginals despite instability of the terminal fixed point.

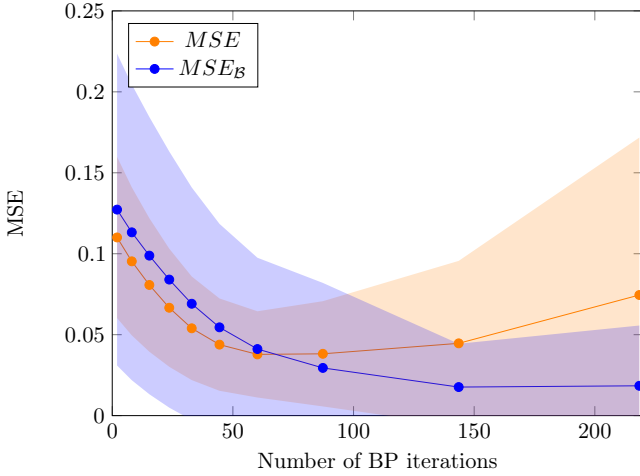


Fig. 2: MSE (orange) and MSE_B (blue) over the cumulative number of iterations. Results are averaged over 100 grid graphs (5×5); $\theta_i = 0.4$ and $J_{ij} \in \{-1, 1\}$.

difference is primarily determined by the number of steps M . Ideally M should be as large as possible. This, however, increases the runtime (cf. Theorem 3); in practice we would choose M as small as possible but as large as necessary. Moreover, one can adaptively increase the step size if two successive fixed points are close, i.e., if $\underline{\mu}_{[m]}^{\circ} \simeq \underline{\mu}_{[m-1]}^{\circ}$ (cf. [29, pp.23], [1]). Our experiments show that it is sufficient to use rather coarse steps; we used $M \leq 10$ for all reported experiments.

Additionally, instead of initializing $\mathcal{BP}_{[m]}$ with its preceding fixed point messages, i.e., $\underline{\mu}_{[m]}^{\circ} = \underline{\mu}_{[m-1]}^{\circ}$ one can (e.g., by spline extrapolation) estimate $\underline{\mu}_{[m]}^{\circ} = f(\underline{\mu}_{[m-1]}^{\circ}, \underline{\mu}_{[m-2]}^{\circ}, \dots, \underline{\mu}_{[m-k]}^{\circ})$ so that $\underline{\mu}_{[m]}^{\circ} \simeq \underline{\mu}_{[m]}^{\circ}$ to reduce the overall number of iterations. We empirically observed that the benefit diminishes for $k > 3$.

3.2 Pseudocode

Pseudocode of SBP is presented in Algorithm 1. The maximum number of iterations for BP is given by $N_{BP} = 10^3$. We randomly initialize $\underline{\mu}^0$ and either use fixed step size or adaptive step size (*adaptive stepsize* = 1). The sequences of messages is contained in $\{\underline{\mu}_{[m]}^{\circ}\} = \{\underline{\mu}_{[1]}^{\circ}, \dots, \underline{\mu}_{[m]}^{\circ}\}$.

Cubic spline extrapolation is applied in `ExtrapolateMsg` to estimate the initial messages of the subsequent model.

We further present the pseudocode for the adaptive step size controller in Algorithm 2.

Algorithm 1: Self-Guided Belief Propagation (SBP)

input : Graph $\mathcal{G} = (\mathbf{X}, \mathbf{E})$, Potentials Ψ

output: Fixed point messages $\underline{\mu}^{\circ}$

```

1 initialization  $\underline{\mu}_{[1]}^{\circ} \leftarrow \underline{\mu}^0$ 
2  $m \leftarrow 1$ 
3  $step_{init} \leftarrow 0.1$ 
4  $\zeta_1 \leftarrow 0$ 
5 while  $\zeta \leq 1$  do
6    $\Psi(\zeta_m) \leftarrow \text{ScalePotentials}(\Psi, \zeta_m)$ 
7    $(\underline{\mu}, iterations) \leftarrow \text{BP}(\underline{\mu}_{[m]}^{\circ}, \Psi(\zeta_m), N_{BP})$ 
8   if  $iterations < N_{BP}$  then
9      $\underline{\mu}_{[m]}^{\circ} \leftarrow \underline{\mu}$ 
10  else
11    break
12  if adaptive stepsize then
13     $\zeta_{m+1} \leftarrow \zeta_m + \text{AdaptiveStepSize}(\{\underline{\mu}_{[m]}^{\circ}\},$ 
14       $step_{init}, m)$ 
15  else
16     $\zeta_{m+1} \leftarrow \zeta_m + step_{init}$ 
17   $\underline{\mu}_{[m+1]}^{\circ} \leftarrow \text{ExtrapolateMsg}(\{\underline{\mu}_{[m]}^{\circ}\}, \{\zeta_m\})$ 
18   $m \leftarrow m + 1$ 
19  $\underline{\mu}^{\circ} \leftarrow \underline{\mu}_{[m-1]}^{\circ}$ 

```

Algorithm 2: Adaptive Step Size Controller

input : Sequence of messages $\{\underline{\mu}_{[m]}^{\circ}\}$, $step_{init}$, m

output: $step$

```

1  $step \leftarrow step_{init}$ 
2  $threshold \leftarrow 1 \cdot 10^{-3}$ 
3  $k \leftarrow 1$ 
4 while  $(\text{MSE}(\underline{\mu}_{[m]}^{\circ}) - \text{MSE}(\underline{\mu}_{[m-k]}^{\circ})) < threshold$  do
5    $k \leftarrow k + 1$ 
6    $step \leftarrow step + step_{init} \cdot k$ 

```

4 EXPERIMENTS

We apply SBP to $n \times n$ grid graphs of different size, complete graphs with $N = 10$ random variables, and random graphs with $N = 10$ random variables and with an average degree of $|\partial(X_i)| = 3$. We consider attractive (Sec. 4.2) and general (Sec. 4.3) models for each of these graphs. Experiments were performed for these graphs in order to make the results comparable to previous work [21], [30], [31], [40].

4.1 Experimental settings

SBP is evaluated and compared to BP, BP_D (BP with damping), and Gibbs sampling. The accuracy is evaluated by the mean squared error (MSE) between the approximate marginals \hat{P}_{X_i} and the exact marginals P_{X_i} , where the exact marginals P_{X_i} are obtained by the Junction Tree algorithm [19]. For binary random variables we can apply symmetry properties so that

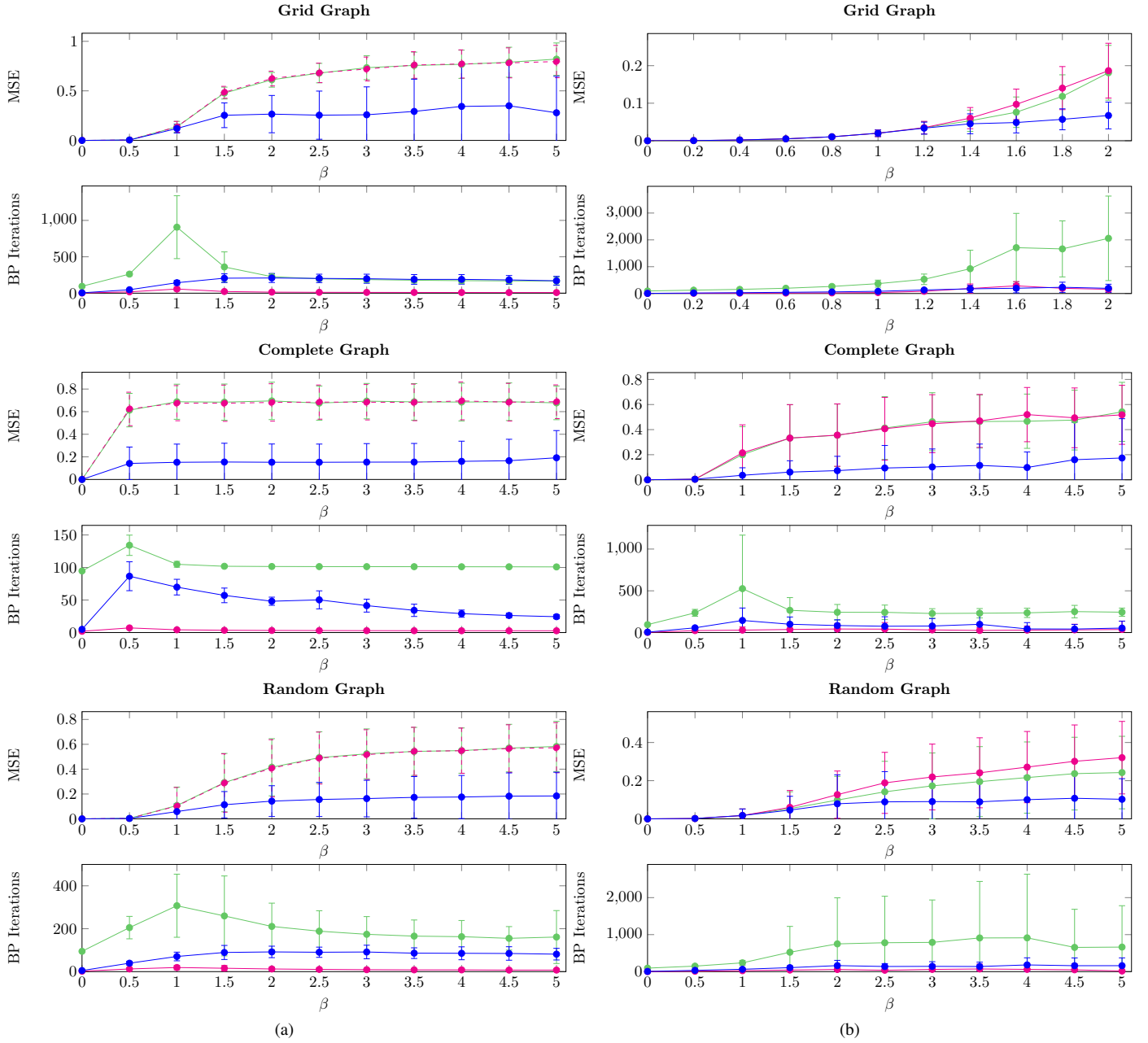


Fig. 3: MSE and number of iterations for: SBP_{all} (blue), BP^o (magenta), and BP_D^o (green); $\theta_i \sim \mathcal{U}(-0.5, 0.5)$ and (a) $J_{ij} \sim \mathcal{U}(0, \beta)$ (attractive model); (b) $J_{ij} \sim \mathcal{U}(-\beta, \beta)$ (general model).

$\text{MSE} = \frac{2}{N} \sum_{i=1}^N |P_{X_i}(+1) - \tilde{P}_{X_i}(+1)|^2$. Additionally, we evaluate $\text{MSE}_{\mathcal{B}}$ between the approximate marginals obtained at $\mathcal{F}_{\mathcal{B}}^{\circ}$ and the marginals obtained at the global minimum $\mathcal{F}_{\mathcal{B}}^*$, where we approximate $\mathcal{F}_{\mathcal{B}}^*$ by [39]. We further compare the runtime of all methods by counting the overall number of BP iterations and the number of iterations for Gibbs sampling.³ We consider $L = 100$ models with random potentials for every experiment. The initial messages are randomly initialized 100 times for each of these L models, before applying BP with and without damping. We consider BP (and BP_D) as converged for a model if at least a single message initialization (out of 100) exists

for which BP converges. We report the convergence ratio, i.e., the number of experiments (or probabilistic graphical models) for which BP converged divided by the overall number of experiments L . SBP, on the other hand, allows to obtain an approximation of the terminal fixed point in case that this fixed point is unstable, which prevents BP and BP_D from converging.

The reported error (MSE) and the number of iterations are averaged over all convergent runs of BP and BP_D (i.e., BP^o and BP_D^o) while all runs that did not converge are discarded. On the contrary, we average the error and the number of iterations over all L models for SBP (SBP_{all}), Gibbs sampling (Gibbs_{all}), and for minimization of the Bethe approximation ($\mathcal{F}_{\mathcal{B}}^*$).

For BP and SBP we set the maximum number of iterations to $N_{BP} = 10^3$ and use random scheduling. For BP_D we choose a

3. Computing the acceptance-probability requires similar runtime as one BP message update

TABLE 1: RESULTS FOR GENERAL MODELS WITH $J_{ij} \in \{-1, 1\}$ ON GRID GRAPHS ($N = 25$ AND $N = 100$), COMPLETE GRAPHS ($N = 10$), AND RANDOM GRAPHS ($N = 10$). WE REPORT THE MSE TO THE EXACT MARGINALS AND THE MSE_B TO THE BETHE APPROXIMATION, CONVERGENCE RATIO, AND THE OVERALL NUMBER OF BP ITERATIONS. ONLY CONVERGED RUNS ARE CONSIDERED FOR BP° AND BP_D° BUT ALL RUNS ARE CONSIDERED FOR SBP_{all} , GIBBS_{all} , AND $\mathcal{F}_{B_{all}}^*$.

	θ	Grid Graph(5×5)			Grid Graph (10×10)			Complete Graph			Random Graph		
		0	0.1	0.4	0	0.1	0.4	0	0.1	0.4	0	0.1	0.4
MSE	BP°	0.338	0.251	0.102	-	-	0.184	0.463	0.466	0.356	0.252	0.202	0.101
	BP_D°	0.226	0.198	0.066	0.186	0.240	0.154	0.463	0.473	0.422	0.128	0.116	0.083
	SBP_{all}	0.000	0.029	0.047	0.000	0.026	0.077	0.000	0.055	0.074	0.000	0.048	0.049
	$\mathcal{F}_{B_{all}}^*$	0.036	0.042	0.069	-	-	-	-	-	-	-	-	-
	Gibbs_{all}	0.001	0.016	0.064	0.001	0.037	0.120	0.096	0.096	0.077	0.001	0.011	0.048
Convergence ratio	BP°	0.05	0.11	0.26	0.00	0.00	0.02	0.41	0.42	0.50	0.30	0.33	0.49
	BP_D°	0.11	0.16	0.69	0.01	0.02	0.12	0.41	0.41	0.50	0.62	0.64	0.80
Number of iterations	BP°	40	52	84	-	-	102	17	17	18	42	53	50
	BP_D°	1370	1449	1735	2711	2313	2599	211	207	234	1077	1057	873
	SBP_{all}	5	182	146	5	149	209	5	51	110	5	149	131
	Gibbs_{all}	10^5	10^5	10^5	10^5	10^5	10^5	10^5	10^5	10^5	10^5	10^5	10^5
MSE_B	SBP_{all}	0.036	0.037	0.022	-	-	-	-	-	-	-	-	-
$\mathcal{F}_{B^\circ}(\zeta_M)$ equals	SBP	100	10	23	-	-	-	-	-	-	-	-	-

large damping factor $\epsilon = 0.9$ to account for the strong couplings and therefore increase the maximum number of iterations to $N_{BP} = 10^4$. Such a large damping factor helps to prioritize convergence over runtime – this admits comparison of marginal accuracy for a wide range of models. Carefully selecting a damping factor that depends on a given model may reduce the number of iterations until convergence but cannot not increase the accuracy; moreover, if chosen too small BP_D may fail to converge at all. The accuracy of SBP is only marginally affected by its parameters and we use the following parameters for all experiments: $M \leq 10$, adaptive step size, and cubic spline extrapolation. Gibbs sampling is run for 10^5 iterations.

4.2 Attractive models

We consider grid graphs with $N = 100$ random variables (10×10), random graphs with $N = 10$ random variables, and complete graphs with $N = 10$ random variables. We generate $L = 100$ models for every value of $\beta \in \{0, 0.5, \dots, 5\}$ and sample the potentials according to $\theta_i \sim \mathcal{U}(-0.5, 0.5)$ and $J_{ij} \sim \mathcal{U}(0, \beta)$; i.e., overall we consider 1100 different parametrizations for each individual graph-structure. Note that BP is initialized 100 times for every considered model. We compute the MSE for every value of β and visualize the mean and the standard deviation of the MSE^4 as well as the number of iterations in Fig. 3a.

Note that BP (magenta) converges rapidly for all graphs considered; hence, there is no additional benefit for BP_D (green) that only increases the number of iterations. SBP (blue) only slightly increases the number of iterations as compared to BP and converges in fewer iterations than BP_D . Note that SBP is guaranteed to capture the global optimum if all local potentials are unidirectional (cf. Theorem 5-6). But even if we do allow for random local potentials, we empirically observe that SBP consistently outperforms BP with respect to accuracy. This becomes especially evident for models with strong couplings: These models exhibit multiple stable fixed points [14] such that, depending on the initialization, BP often converges to inaccurate fixed points.

4. Note that the MSE is not Gaussian distributed but we report the standard deviation for simplicity.

4.3 General models

General models traditionally pose problems for BP and other methods that aim to minimize the Bethe approximation.

First, in order to evaluate the performance of SBP we consider $\theta_i = \theta \in \{0, 0.1, 0.4\}$ and draw the couplings with equal probability from $J_{ij} \in \{-1, 1\}$; the results are summarized in Tab. 1. Although BP and BP_D fail to converge for most models we observe that SBP stops after only a few iterations and significantly outperforms BP in terms of accuracy. In fact, SBP achieves accuracy competitive with Gibbs sampling but requires three orders of magnitude fewer iterations.

Second, we further apply SBP to general graphs and evaluate whether SBP provides a good approximation of the pseudomarginals $\tilde{P}_{\mathbf{X}_B}^*$ that correspond to the global minimum of the Bethe free energy \mathcal{F}_B^* . Therefore we consider grid graphs (of size 5×5), which still allows us to approximate \mathcal{F}_B^* – and the related pseudomarginals $\tilde{P}_{\mathbf{X}_B}^*$ – reasonable well by [39]. The results are summarized in Tab. 1 and show that SBP approximates $\tilde{P}_{\mathbf{X}_B}^*$ within the accuracy of our reference method (MSE_B). We further report the number of times where SBP obtains the terminal fixed point, i.e., for \mathcal{U}_M , in Tab. 1 ($\mathcal{F}_{B^\circ}(\zeta_M)$ equals SBP). It becomes obvious that SBP approximates the terminal fixed point reasonably well, despite frequently stopping for $\zeta_m < 1$. Moreover, looking at the MSE reveals that SBP does not only approximate the pseudomarginals $\tilde{P}_{\mathbf{X}_B}^*$ well, but concurrently provides an accurate approximation of the exact marginals $P_{\mathbf{X}_B}$.

Third, we investigate how the approximation quality depends on the scaling parameter ζ_m . Therefore, we depict the evolution of the MSE (to the exact solution) and MSE_B (to the approximate solution) in Fig. 2. We observe that MSE_B (blue) decreases monotonically with every iteration, which empirically verifies that SBP proceeds along a well-behaved solution path (cf. Prop. 1). Note that MSE_B decreases rapidly in the first iterations and SBP spends a major part of the overall runtime for slight improvements. The MSE to the exact solution, on the other hand, decreases first until it increases again as SBP incorporates stronger couplings. Stronger couplings tend to degrade the quality of the Bethe approximation in loopy graphs and lead to marginals that are increasingly biased

towards one state [14], [37]. This explains why the MSE to the exact solution increases as SBP converges towards the terminal fixed point. One could exploit this behavior and restrict the runtime by stopping SBP after consumption of a fixed iteration budget; this may even increase the accuracy with respect to the exact solution.

Finally, we aim to investigate the influence of the coupling strength: therefore we consider $\theta_i \sim \mathcal{U}(-0.5, 0.5)$ and $J_{ij} \sim \mathcal{U}(-\beta, \beta)$. For every $\beta \in [0, 5]$ we execute $L = 100$ experiments and present the averaged results in Fig. 3b. Note that we restrict the results to $\beta \leq 2$ on the grid graph because BP did only converge sporadically for models with stronger couplings. SBP requires only slightly more iterations than BP and fewer than BP_D , even though we compare only to models where BP (or BP_D) converged. The benefits of SBP become increasingly evident as the coupling strength increases. Again SBP (blue) significantly outperforms BP° (magenta) and BP_D° (green) on all graphs with respect to accuracy.

5 THEORETICAL PROPERTIES

Here we present some more formal arguments and discuss the properties of SBP to understand under which conditions the algorithm (presented in Sec. 3) can be expected to perform well. We refer to Sec. 6 for the proofs and only present the most important Theorems as well as their implications below.

5.1 Definitions

First, we fix our notation: we denote the pseudomarginals of \mathcal{U}_m by $\tilde{P}_{\mathbf{X}_B}^\circ = \tilde{P}_{\mathbf{X}_B}^\circ(\zeta_m)$, and, with slight abuse of notation, we refer to the corresponding stationary point of the Bethe free energy by $\mathcal{F}_B^\circ(\zeta_m) = \mathcal{F}_B(\tilde{P}_{\mathbf{X}_B}^\circ(\zeta_m))$. It is beneficial to study the behavior of SBP as M tends towards infinity. Therefore we consider the unit interval $\zeta \in [0, 1]$ to be the compact support of the functions $\mathcal{F}_B(\zeta)$ and $\tilde{P}_{\mathbf{X}_B}(\zeta)$. SBP is inspired by the idea to proceed along a so-called *solution path* as ζ increases from zero to one in order to obtain the marginal distributions for the model of interest. Therefore, we shall consider a continuous homotopy function $H(\underline{\mu}, \zeta) : \mathbb{R}^{|\underline{\mu}|+1} \rightarrow \mathbb{R}^{|\underline{\mu}|}$ that is defined by

$$H(\underline{\mu}, \zeta) = \underline{\mu} - \mathcal{BP}(\underline{\mu}) \quad \text{where} \quad \Psi = \Psi(\zeta). \quad (19)$$

Then, a *solution path*

$$c(\zeta) : H(\underline{\mu}, \zeta) = 0 \quad (20)$$

exists that (i) has a start point $c(\zeta = 0) = \underline{\mu} : H(\underline{\mu}, \zeta = 0) = 0$, (ii) an endpoint $c(\zeta = 1) = \underline{\mu} : H(\underline{\mu}, \zeta = 1) = 0$, and (iii) is continuous over $\zeta \in [0, 1]$, i.e., it connects the start- with the endpoint. SBP then proceeds along some solution path from a given start- to its endpoint. Note that the solution path $c(\zeta)$ explicitly defines the pseudomarginals $\tilde{P}_{\mathbf{X}_B}^\circ(\zeta)$ by (9)-(10). In particular, we refer to the start- and end-point by $\tilde{P}_{\mathbf{X}_B}^\circ(\zeta = 0)$ and $\tilde{P}_{\mathbf{X}_B}^\circ(\zeta = 1)$ respectively. The following example in Fig. 4 illustrates the solution set of a grid graph with attractive edges. This example exhibits a unique solution path according to our definition; note, however, that a second curve exists, which lacks a start point and is therefore of no relevance for any method that proceeds along a solution path defined by the homotopy in (19).

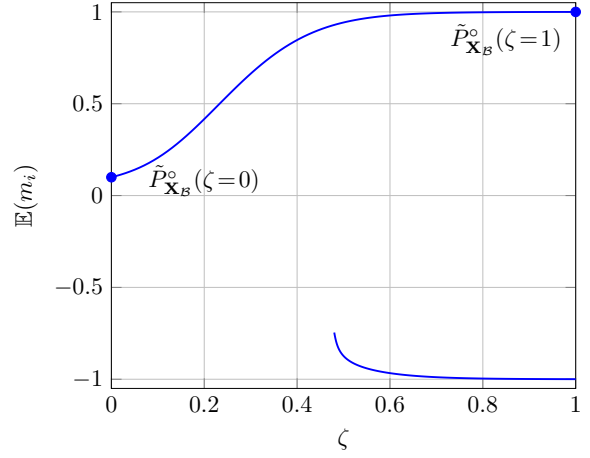


Fig. 4: Solution path (cf. 5.1) for a grid graph; start- and end-point are depicted by blue points. Note how Prop. 1.1-2 are fulfilled.

5.2 Properties of SBP

The following proposition summarizes the main properties of the solution path that is specified and followed by SBP.

Proposition 1 (Properties for attractive and general models).

- (1) *BP has a unique fixed point $\underline{\mu}_{[1]}^* = \underline{\mu}_{[1]}^\circ$ for $\zeta_1 = 0$, i.e., SBP admits a single start point $\tilde{P}_{\mathbf{X}_B}^\circ(\zeta = 0) = \tilde{P}_{\mathbf{X}_B}^\circ(\zeta = 0)$. (cf. Theorem 1)*
- (2) *A smooth (i.e., continuous) solution path originates from $\tilde{P}_{\mathbf{X}_B}^\circ(\zeta = 0)$. (cf. Theorem 2)*
- (3) *SBP efficiently proceeds along this solution path. (cf. Theorem 3)*

Theorem 1 (Prop. 1.1). *A unique solution exists for $\zeta = 0$, i.e., a single start point $\tilde{P}_{\mathbf{X}_B}^\circ(\zeta = 0)$ exists, and BP is guaranteed to converge. Moreover, this start point is exact, i.e., $\tilde{P}_{\mathbf{X}_B}^\circ(\zeta = 0) = P_{\mathbf{X}_B}(\zeta = 0)$.*

This concurs with the sandwich-bound [38, Th.4] that reduces to $P_{X_i}(+1) = \theta_i / (e^{\theta_i} + e^{-\theta_i}) = \tilde{P}_{X_i}(+1)$ for $J_{ij} = 0$. Theorem 1 thus reduces the problem of initializing SBP to computing $\underline{\mu}_{[1]}^*$, which can be done in linear time.

Theorem 2 (Prop. 1.2). *Let $\tilde{P}_{\mathbf{X}_B}^\circ(\zeta)$ be the pseudomarginals that are uniquely defined along the solution path that originates from $\tilde{P}_{\mathbf{X}_B}^\circ(\zeta = 0)$. Then, $\tilde{P}_{\mathbf{X}_B}^\circ(\zeta)$ and the associated stationary point $\mathcal{F}_B^\circ(\zeta)$ are continuous on their compact support $\zeta \in [0, 1]$.*

Theorem 2 substantiates the claim that a smooth solution path emerges from the simple problem (cf. Prop 1.2).

Theorem 3 (Prop. 1.3). *There exists some $\zeta_m \leq 1$ so that SBP converges to $\tilde{P}_{\mathbf{X}_B}^\circ(\zeta_m) \in \mathcal{L}$ in $\mathcal{O}(MN_{BP})$.*

SBP is consequently capable of efficiently tracking the fixed point that emerges as ζ increases and requires MN_{BP} iterations at most. SBP may, however, only converge to a surrogate model for $\zeta_m < 1$ and is not guaranteed to obtain the pseudomarginals of the desired problem. One can characterize this error by computing a bound on $|\mathcal{F}_B^\circ(\zeta_m) - \mathcal{F}_B^\circ(\zeta_M)|$ given the difference between $\Psi_{[m]}$ and $\Psi_{[M]}$ (cf. [12, Th.16]).

Corollary 3.1. *SBP obtains the pseudomarginals of the desired problem if and only if the endpoint $\tilde{P}_{\mathbf{X}_B}^\circ(\zeta = 1)$ is stable. This*

is an immediate consequence of the fact that the convergence properties can only degrade along a given solution path [15].

Prop. 1 is of fundamental importance, but does not relate to the accuracy of the obtained stationary point. Assessing the quality of the Bethe approximation and the accuracy of BP for general models is still an open research question that is beyond the scope of this work. However, we further present Prop. 2 to discuss the accuracy of the obtained solution for *attractive* models.

Proposition 2 (Properties for attractive models with unidirectional fields). *The solution path $c(\zeta)$ leads towards an accurate solution with $\tilde{P}_{\mathbf{X}_B}^\circ(\zeta_m) = \tilde{P}_{\mathbf{X}_B}^*(\zeta_m)$ and $\mathcal{F}_B(\tilde{P}_{\mathbf{X}_B}^\circ(\zeta_m)) = \mathcal{F}_B(\tilde{P}_{\mathbf{X}_B}^*(\zeta_m))$. (cf. Theorem 5-6)*

We start by generalizing Griffiths' inequality [8] to the fixed points of BP (Lemma 4) and subsequently provide Theorem 5-6 that discuss the accuracy of the fixed point obtained by SBP.

Lemma 4. *Consider two attractive probabilistic graphical models \mathcal{U}_0 and \mathcal{U}_1 with equal \mathcal{G} and with all potentials specified by $\theta_i > 0$ and by $J_{ij,0}$ and $J_{ij,1}$, where $J_{ij,0} < J_{ij,1}$ for all $e_{ij} \in \mathbf{E}$. Let us consider a fixed point of BP with positive mean $m_{i,0}^\circ \in (0, 1]$. Then, $m_{i,0}^\circ < m_{i,1}^\circ$ and $\chi_{i,0}^\circ < \chi_{i,1}^\circ$.*

Theorem 5 (Prop. 2). *Consider an attractive model with $\theta_i > 0$.⁵ Then, $m_i^\circ(\zeta)$ increases monotonically along the solution path $c(\zeta)$; in particular SBP minimizes the Bethe approximation error and is optimal with respect to marginal accuracy, i.e.,*

$$\begin{aligned} \tilde{P}_{\mathbf{X}_B}^\circ(\zeta) &= \operatorname{argmin}_{\tilde{P}_{\mathbf{X}_B}^\circ(\zeta) \in \mathcal{L}} |\mathcal{F}_B(\tilde{P}_{\mathbf{X}_B}^\circ(\zeta)) - \mathcal{F}^*| \\ &= \operatorname{argmin}_{\tilde{P}_{\mathbf{X}_B}^\circ(\zeta) \in \mathcal{L}} |\tilde{P}_{\mathbf{X}_B}^\circ(\zeta) - \tilde{P}_{\mathbf{X}_B}^*(\zeta)|. \end{aligned} \quad (21)$$

Theorem 6 (Prop. 2). *Consider an attractive model with $\theta_i = 0$. Then, SBP obtains the exact solution $\tilde{P}_{\mathbf{X}_B}^\circ(\zeta = 1) = P_{\mathbf{X}_B}(\zeta = 1)$.*

To conclude, for attractive models with $\theta_i \leq 0$ or $\theta_i \geq 0$, SBP either obtains the fixed point that corresponds to the global minimum \mathcal{F}_B^* (Theorem 5), or it obtains the fixed point that corresponds to the exact solution, i.e., to \mathcal{F}^* (Theorem 6). For *general models* m_i° need not increase monotonically along the solution path and it is not obvious whether SBP obtains the most accurate fixed point. However, the experimental results in Sec. 4.3 at least corroborate Prop. 1.3 that SBP does often converge to accurate fixed points.

6 DERIVATIONS OF SECTION 5

This Section contains all the detailed proofs for Sec. 5.

6.1 Proofs for Proposition 1

Proof [of Theorem 1]: First, let us obtain the singleton marginals $\tilde{P}_{X_i}(x_i) = \sum_{x_j \in \mathbb{S}} \tilde{P}_{X_i, X_j}(x_i, x_j)$. For $\Phi_{X_i, X_j}(x_i, x_j)_{[1]} = 1$ it follows that marginalizing over (10) equates to

$$\begin{aligned} \tilde{P}_{X_i}(x_i) &= \Phi_{X_i}(x_i) \prod_{X_k \in \{\partial(X_i) \setminus X_j\}} \mu_{ki}^\circ(x_i) \\ &\cdot \sum_{x_j \in \mathbb{S}} \Phi_{X_j}(x_j) \prod_{X_l \in \{\partial(X_j) \setminus X_i\}} \mu_{lj}^\circ(x_j). \end{aligned} \quad (22)$$

5. Note that equal results can be obtained for $\theta_i < 0$ because of symmetry properties.

Note that according to (6) $\mu_{ji}^\circ(x_i)$ is equivalent to the second line of (22) so that

$$\tilde{P}_{X_i}(x_i) = \Phi_{X_i}(x_i) \prod_{X_k \in \partial(X_i)} \mu_{ki}^\circ(x_i), \quad (23)$$

which equals (9). It follows that $\tilde{P}_{X_i}(+1) = e^{\theta_i} / (e^{\theta_i} + e^{-\theta_i}) = P_{X_i}(+1)$. \square

Proof [of Theorem 2]: First we show that the Bethe free energy $\mathcal{F}_B(\zeta)$ itself is an analytic function. Consider (15) with the pairwise potentials defined by (17). Then, the derivative with respect to ζ is given by

$$\begin{aligned} \frac{\partial \mathcal{F}_B(\zeta)}{\partial \zeta} &= -\frac{\partial}{\partial \zeta} \sum_{e_{ij} \in \mathbf{E}} \sum_{x_i, x_j} \tilde{P}_{X_i, X_j}(x_i, x_j) \ln \Phi_{X_i, X_j}(x_i, x_j) \\ &= -\frac{\partial}{\partial \zeta} \sum_{e_{ij} \in \mathbf{E}} \sum_{x_i, x_j} \tilde{P}_{X_i, X_j}(x_i, x_j) \cdot \zeta J_{ij} \cdot x_i x_j \\ &= -\sum_{e_{ij} \in \mathbf{E}} J_{ij} \cdot \chi_{ij}. \end{aligned} \quad (24)$$

As an immediate consequence we observe that $\mathcal{F}_B(\zeta)$ is continuously differentiable⁶ as (24) is a finite sum over finite terms.⁷

We specifically consider $\mathcal{F}_B^\circ(\zeta)$ that emerges from $\mathcal{F}_B^\circ(\zeta = 0) = \mathcal{F}_B^*(\zeta = 0)$; this start point is unique by Theorem 1. It follows by (24) that $\mathcal{F}_B^\circ(\zeta)$ varies in a continuous fashion along the unique solution path for $\zeta \in [0, 1]$. Further note that stationary points are in a one-to-one correspondence with fixed points of BP which completes the proof.

Further note that the set of stationary points is finite [36]⁸ and that pitchfork bifurcations may only occur if $\theta_i = 0$ [14], [26], in which case SBP obtains the exact solution (cf. Theorem 5). \square

Proof [of Theorem 3]: SBP increases ζ_m as long as BP converges in less than N_{BP} iterations, and stops otherwise. Consequently, BP corrects the accuracy of the fixed point for each value ζ_m within a bounded number of iterations. The runtime of SBP is further determined by the choice of M , i.e., the step-size (cf. Sec. 3.1). Assume that SBP converges for ζ_m , then it does so in $\mathcal{O}(M \cdot N_{BP})$. \square

6.2 Proofs for Proposition 2

Proof [of Lemma 4]: Essentially, we first show that $\mu_{ij}(X_j = 1) / \mu_{ij}(X_j = -1)$ increases monotonically with J_{ij} and then express the pseudomarginals in terms of (9) and (10).

Let us denote the messages on \mathcal{U}_0 and on \mathcal{U}_1 by $\mu_{ij}(x_j)_0$ and $\mu_{ij}(x_j)_1$ respectively. Further, let all local potentials $\theta_i > 0$, and let all pairwise potentials of \mathcal{U}_1 be ϵ -larger than those of \mathcal{U}_0 , i.e., $0 < J_{ij,0} = J_{ij,1} - \epsilon$. Note that by assumption $m_i \in (0, 1]$ so that

$$\mu_{ij}(X_j = +1) \geq \mu_{ij}(X_j = -1). \quad (25)$$

First, we show that for all $e_{ij} \in \mathbf{E}$

$$\frac{\mu_{ij}^\circ(X_j = +1)_0}{\mu_{ij}^\circ(X_j = -1)_0} < \frac{\mu_{ij}^\circ(X_j = +1)_1}{\mu_{ij}^\circ(X_j = -1)_1}. \quad (26)$$

6. Strictly speaking $\mathcal{F}_B(\zeta)$ is an analytic function.

7. This is in accordance with the fact that true phase transitions (singularities in the derivative of the free energy) can occur only in the thermodynamic limit, where (24) is an infinite sum that equates to infinity.

8. This is also required for the one-step replica symmetry breaking assumption [22, Sec.19].

Therefore, consider the update rule of (6) for both states

$$\begin{aligned} \mu_{ij}^{n+1}(X_j = +1)_1 &\propto e^{J_{ij} + \theta_i + \epsilon} \prod_{X_k \in \{\partial(X_i) \setminus X_j\}} \mu_{ki}^n(X_i = +1)_1 \\ &+ e^{-J_{ij} - \theta_i - \epsilon} \prod_{X_k \in \{\partial(X_i) \setminus X_j\}} \mu_{ki}^n(X_i = -1)_1, \end{aligned} \quad (27)$$

and

$$\begin{aligned} \mu_{ij}^{n+1}(X_j = -1)_1 &\propto e^{-J_{ij} + \theta_i - \epsilon} \prod_{X_k \in \{\partial(X_i) \setminus X_j\}} \mu_{ki}^n(X_i = +1)_1 \\ &+ e^{J_{ij} - \theta_i + \epsilon} \prod_{X_k \in \{\partial(X_i) \setminus X_j\}} \mu_{ki}^n(X_i = -1)_1. \end{aligned} \quad (28)$$

In (27) the larger product is multiplied by e^ϵ and the smaller product is divided by e^ϵ . For (28) it is exactly the other way round so that the ratio between the messages increases which proofs (26). We shall denote the imposed difference $\delta \in \mathbb{R}_+^*$ on the messages by

$$\mu_{ij}^\circ(X_j = +1)_1 = \mu_{ij}^\circ(X_j = +1)_0 + \delta, \quad (29)$$

$$\mu_{ij}^\circ(X_j = -1)_1 = \mu_{ij}^\circ(X_j = -1)_0 - \delta. \quad (30)$$

Second, we show that $m_{i,0}^\circ < m_{i,1}^\circ$ which is an immediate consequence of plugging (29) and (30) into (9).

Finally, it remains to show that $0 < \overset{(i)}{\chi}_{ij,0} < \overset{(ii)}{\chi}_{ij,1}$. Without loss of generality we assume that all variables have equal degree $d + 1$ and constant coupling strength $J_{ij} = J$. First we show that (i) holds, i.e., $\chi := \chi_{ij,0}^\circ$ is positive. Let us express the marginals by (10) and denote the messages by $\mu := \mu_{ij}(X_j = 1)_0$. It follows that $\mu_{ij}(X_j = -1)_0 = (1 - \mu)$ and that

$$\chi = e^{J+2\theta} \mu^{2d} + e^{J-2\theta} (1-\mu)^{2d} - 2e^{-J} \mu^d (1-\mu)^d. \quad (31)$$

Let us further represent the messages by $\mu = 1/2 + x$ with $x \in [0, 1/2]$. It follows that

$$\begin{aligned} \chi &\stackrel{(a)}{\geq} \left((1/2 + x)^{2d} + (1/2 - x)^{2d} \right) \\ &\quad - 2(1/2 + x)^d (1/2 - x)^d \end{aligned} \quad (32)$$

$$= \left((1/2 - x)^d - (1/2 + x)^d \right)^2 \quad (33)$$

$$\stackrel{(b)}{\geq} 0, \quad (34)$$

where (a) follows from neglecting all exponential terms and thus upper bounding the positive term and lower bounding the negative term (with equality if and only if $J = 0$ and $\theta = 0$) and (b) is a direct consequence of the square in (33). Now let us show that (ii) holds, i.e., χ increases monotonically, by taking the derivative of (31), so that

$$\begin{aligned} \frac{\partial}{\partial \mu} \chi &= 2d \left(e^{J+2\theta} \mu^{2d-1} - e^{J-2\theta} (1-\mu)^{2d-1} \right) \\ &\quad + 2de^{-J} \left(\mu^d (1-\mu)^{d-1} - \mu^{d-1} (1-\mu)^d \right) \end{aligned} \quad (35)$$

$$\stackrel{(a)}{\geq} 2de^{-J} \left(\mu^d (1-\mu)^{d-1} - \mu^{d-1} (1-\mu)^d \right) \quad (36)$$

$$\stackrel{(b)}{\geq} 0, \quad (37)$$

where (a) follows from neglecting the, strictly positive, first term in (35), and (b) is a direct consequence from (25). \square

Proof [of Theorem 5]: A unique start point $\tilde{P}_{\mathbf{X}_B}^\circ(\zeta = 0)$ exists by Theorem 1 that equals the exact pseudomarginals $P_{\mathbf{X}_B}(\zeta = 0)$ and, for $\theta_i > 0$, has positive mean and correlation), i.e., $m_i^*(\zeta = 0) = m_i^\circ(\zeta = 0) > 0$.

Consequently, Lemma 4 applies, which further implies that $m_i^\circ(\zeta)$ and $\chi_{ij}^\circ(\zeta)$ are monotonically increasing; moreover, $m_i^\circ(\zeta)$ and $\chi_{ij}^\circ(\zeta)$ are continuous by Theorem 2. In particular, this further implies that the Bethe free energy $\mathcal{F}_B^\circ(\zeta)$ is monotonically decreasing. This further implies that the Bethe free energy $\mathcal{F}_B^\circ(\zeta)$ decreases. Let $\mathcal{F}_B^\circ(\zeta = 1)$ correspond to the endpoint of the solution path $c(\zeta)$ that emerges from the origin; then, it immediately follows that the error with respect to the endpoint $\mathcal{F}_B^\circ(\zeta = 1)$ decreases along the solution path: i.e., consider two arbitrary values $m, k \in [0, 1]$ such that $k > m$, then $|\mathcal{F}_B^\circ(\zeta_m) - \mathcal{F}_B^\circ(\zeta = 1)| \geq |\mathcal{F}_B^\circ(\zeta_k) - \mathcal{F}_B^\circ(\zeta = 1)|$.

It remains to show that SBP obtains the fixed point $\mathcal{F}_B^\circ(\zeta = 1)$ that minimizes the error with respect to the exact free energy $\mathcal{F}^*(\zeta = 1)$. Therefore consider the fact, that attractive models with $\theta_i > 0$ have a unique fixed point that satisfies $m_i^\circ(\zeta) \in (0, 1]$ [43]. A second minimum with negative means may, however, emerge for sufficiently large values of J_{ij} . We denote this alternative stationary point by \mathcal{F}_B^\oplus . This minimum \mathcal{F}_B^\oplus , if it exists, is close to being symmetric with $m_i^\oplus(\zeta) + \epsilon = -m_i^\circ(\zeta)$ and $\chi_{ij}^\oplus(\zeta) + \epsilon = \chi_{ij}^\circ(\zeta)$.

Now let us express the Bethe free energy in (15) of both fixed points $\tilde{P}_{\mathbf{X}_B}^\circ$ and $\tilde{P}_{\mathbf{X}_B}^\oplus$ in terms of their energy and entropy by $\mathcal{F}_B = E_B - S_B$ (cf. Sec. 2.4). Then, as a consequence of symmetry of the entropy $S_B(\tilde{P}_{\mathbf{X}_B}^\oplus) \cong S_B(\tilde{P}_{\mathbf{X}_B}^\circ)$ and as a consequence of singleton marginals that are not aligned to the local potentials in (13) $E_B(\tilde{P}_{\mathbf{X}_B}^\oplus) > E_B(\tilde{P}_{\mathbf{X}_B}^\circ)$. It follows that $\mathcal{F}_B(\tilde{P}_{\mathbf{X}_B}^\oplus) \geq \mathcal{F}_B(\tilde{P}_{\mathbf{X}_B}^\circ) = \mathcal{F}_B^*$ (cf. [26]).

That is, SBP proceeds along a solution path that leads towards the global minimum of the Bethe approximation. In particular, by considering the fact that the exact free energy is upper bounded by the Bethe approximation for attractive models [27], this implies that the obtained fixed point indeed minimizes the approximation error $|\mathcal{F}_B(\tilde{P}_{\mathbf{X}_B}^\circ(\zeta)) - \mathcal{F}^*|$ over the local polytope \mathcal{L} .

This concurrently implies that $\tilde{P}_{\mathbf{X}_B}^\circ(\zeta)$ is optimal with respect to marginal accuracy, i.e., no stable fixed point – which corresponds to a local minimum of the Bethe free energy – exists that provides more accurate marginals. Note that attractive models exhibit so-called replica symmetric solutions where the Bethe free energy has two minima at most. In particular, this allows one to express the exact marginals as a convex combination of all fixed points, i.e., $P_{\mathbf{X}_B} = \sum \tilde{P}_{\mathbf{X}_B}^\circ \cdot \exp(-\mathcal{F}_B(\tilde{P}_{\mathbf{X}_B}^\circ))$ [22, Ch.17]. It follows by the existence of at most two solutions that the fixed point that minimizes the Bethe free energy is also more accurate. \square

Proof [of Theorem 6]: Restricting to attractive models makes it straightforward to calculate the exact solution if all $\theta_i = 0$. The exact solution always has zero mean for all random variables, i.e., $m_i(\zeta) = 0$ for all possible values of ζ . This further corresponds to a stationary point $\mathcal{F}_B^\circ(\zeta)$ [23] that constitutes the global minimum $\mathcal{F}_B^*(\zeta)$ for sufficiently small values of J_{ij} but turns into a local maximum for large J_{ij} [22, pp.385]. SBP consistently obtains this solution nonetheless: it follows by Theorem 1 that $m_i^\circ(\zeta = 0) = 0$ and that all messages are equal, i.e., $\mu_{[1]}^*(\zeta = 0) = 1/2$ for all $e_{ij} \in \mathbf{E}$. SBP remains exactly on this fixed point, and obtains the exact marginals as these fixed point messages can be represented exactly, without

any quantization errors in binary arithmetic. \square

7 CONCLUSION

In this paper we introduced an iterative algorithm to perform approximate inference: self-guided belief propagation (SBP) is a simple and robust method that gradually accounts for the pairwise potentials and guides itself towards a unique, stable, and accurate solution. We provide a comprehensive theoretical analysis and substantiate the results empirically in order to validate the underlying assumptions: (i) a smooth solution path exists and originates from the unique fixed point that is obtained by neglecting the pairwise potentials. (ii) This solution path is well-behaved and can be tracked efficiently. (iii) The solution of SBP approximates the exact solution well and corresponds to the global optimum of the Bethe approximation for attractive models with unidirectional local potentials.

Overall SBP significantly improves the accuracy in our experiments on attractive and general models. The obtained marginals are consistently better than for BP with and without damping. Moreover, SBP approximates the exact marginals well on graphical models for which BP does not converge at all.

REFERENCES

- [1] E. Allgower and K. Georg. *Introduction to Numerical Continuation Methods*. Society for Industrial and Applied Mathematics, 2003.
- [2] A. Braunstein, F. Kayhan, G. Montorsi, and R. Zecchina. Encoding for the blackwell channel with reinforced belief propagation. In *IEEE International Symposium on Information Theory*, 2007.
- [3] V. Chandrasekaran, M. Chertkov, D. Gamarnik, D. Shah, and J. Shin. Counting independent sets using the Bethe approximation. *SIAM Journal on Discrete Mathematics*, 25(2):1012–1034, 2011.
- [4] G. F. Cooper. The computational complexity of probabilistic inference using Bayesian belief networks. *Artificial intelligence*, 42(2-3):393–405, 1990.
- [5] A. Dembo and A. Montanari. Ising models on locally tree-like graphs. *The Annals of Applied Probability*, 20(2):565–592, 2010.
- [6] G. Elidan, I. McGraw, and D. Koller. Residual belief propagation: Informed scheduling for asynchronous message passing. In *Proceedings of UAI*, pages 165–173, 2006.
- [7] A. Globerson and T. Jaakkola. Convergent propagation algorithms via oriented trees. In *Proceedings of UAI*, 2007.
- [8] R. B. Griffiths. Correlations in Ising ferromagnets. ii. external magnetic fields. *Journal of Mathematical Physics*, 8(3):484–489, 1967.
- [9] T. Hazan and A. Shashua. Convergent message-passing algorithms for inference over general graphs with convex free energies. In *Proceedings of UAI*, 2008.
- [10] T. Heskes. On the uniqueness of loopy belief propagation fixed points. *Neural Computation*, 16(11):2379–2413, 2004.
- [11] A. Ihler. personal communication, UAI, 2017-08-12.
- [12] A. Ihler, J. Fisher, and A. Willsky. Loopy belief propagation: convergence and effects of message errors. In *Journal of Machine Learning Research*, pages 905–936, 2005.
- [13] M. Jordan. Graphical models. *Statistical Science*, pages 140–155, 2004.
- [14] C. Knoll, D. Mehta, T. Chen, and F. Pernkopf. Fixed Points of Belief Propagation—An Analysis via Polynomial Homotopy Continuation. *IEEE Trans. on Pattern Analysis and Machine Intelligence*, 2017.
- [15] C. Knoll and F. Pernkopf. On Loopy Belief Propagation—Local Stability Analysis for Non-Vanishing Fields. In *Proceedings of UAI*, 2017.
- [16] C. Knoll, M. Rath, S. Tschiatschek, and F. Pernkopf. Message Scheduling Methods for Belief Propagation. In *Machine Learning and Knowledge Discovery in Databases*, pages 295–310. Springer, 2015.
- [17] D. Koller and N. Friedman. *Probabilistic Graphical Models: Principles and Techniques*. MIT press, 2009.
- [18] F. Kschischang, B. Frey, and H. Loeliger. Factor graphs and the sum-product algorithm. *IEEE Trans. on Information Theory*, 47(2):498–519, 2001.
- [19] S. Lauritzen and D. Spiegelhalter. Local computations with probabilities on graphical structures and their application to expert systems. *Journal of the Royal Statistical Society*, pages 157–224, 1988.
- [20] T. Meltzer, A. Globerson, and Y. Weiss. Convergent message passing algorithms: a unifying view. In *Proceedings of UAI*, pages 393–401, 2009.
- [21] O. Meshi, A. Jaimovich, A. Globerson, and N. Friedman. Convexifying the Bethe free energy. In *Proceedings of UAI*, pages 402–410, 2009.
- [22] M. Mezard and A. Montanari. *Information, Physics, and Computation*. Oxford Univ. Press, 2009.
- [23] J. M. Mooij and H. J. Kappen. Sufficient conditions for convergence of the sum–product algorithm. *IEEE Trans. on Information Theory*, 53(12):4422–4437, 2007.
- [24] K. Murphy, Y. Weiss, and M. Jordan. Loopy belief propagation for approximate inference: an empirical study. In *Proceedings of UAI*, pages 467–475, 1999.
- [25] F. Pernkopf, R. Peharz, and S. Tschiatschek. *Introduction to Probabilistic Graphical Models*. Academic Press’ Library in Signal Processing, 2014.
- [26] X. Pitkow, Y. Ahmadian, and K. D. Miller. Learning unbelievable probabilities. In *NIPS*, pages 738–746, 2011.
- [27] N. Ruozzi. Beyond log-supermodularity: lower bounds and the bethe partition function. In *Proceedings of UAI*, pages 546–555, 2013.
- [28] J. Shin. Complexity of Bethe Approximation. In *Proceedings of AISTATS*, pages 1037–1045, 2012.
- [29] A. Sommese and C. Wampler. *The Numerical Solution of Systems of Polynomials Arising in Engineering and Science*, volume 99. World Scientific, 2005.
- [30] D. Sontag and T. S. Jaakkola. New outer bounds on the marginal polytope. In *NIPS*, pages 1393–1400, 2008.
- [31] C. Srinivasa, S. Ravanbakhsh, and B. Frey. Survey Propagation beyond Constraint Satisfaction Problems. In *Proceedings of AISTATS*, pages 286–295, 2016.
- [32] C. Sutton and A. McCallum. Improved dynamic schedules for belief propagation. In *Proceedings of UAI*, pages 376–383, 2007.
- [33] S. C. Tatikonda and M. I. Jordan. Loopy belief propagation and Gibbs measures. In *Proceedings of UAI*, pages 493–500, 2002.
- [34] M. J. Wainwright, T. S. Jaakkola, and A. S. Willsky. Tree-reweighted belief propagation algorithms and approximate ml estimation by pseudomoment matching. In *Proceedings of AISTATS*, 2003.
- [35] M. J. Wainwright, M. I. Jordan, et al. Graphical models, exponential families, and variational inference. *Foundations and Trends in Machine Learning*, 1(1–2):1–305, 2008.
- [36] Y. Watanabe and K. Fukumizu. Graph zeta function in the Bethe free energy and loopy belief propagation. In *NIPS*, pages 2017–2025, 2009.
- [37] Y. Weiss. Correctness of local probability propagation in graphical models with loops. *Neural Comp.*, 12(1), 2000.
- [38] A. Weller and T. Jebara. Bethe bounds and approximating the global optimum. In *Proceedings of AISTATS*, pages 618–631, 2013.
- [39] A. Weller and T. Jebara. Approximating the Bethe partition function. In *Proceedings of UAI*, pages 858–867, 2014.
- [40] A. Weller, K. Tang, T. Jebara, and D. Sontag. Understanding the bethe approximation: when and how can it go wrong? In *Proceedings of UAI*, pages 868–877, 2014.
- [41] M. Welling and Y. Teh. Approximate inference in Boltzmann machines. *Artificial Intelligence*, 143(1):19–50, 2003.
- [42] A. S. Willsky, E. B. Sudderth, and M. J. Wainwright. Loop series and Bethe variational bounds in attractive graphical models. In *NIPS*, pages 1425–1432, 2008.
- [43] J. S. Yedidia, W. T. Freeman, and Y. Weiss. Constructing free-energy approximations and generalized belief propagation algorithms. *IEEE Trans. on Information Theory*, 51(7):2282–2312, 2005.
- [44] A. Yuille and A. Rangarajan. The concave-convex procedure. *Neural Computation*, 15(4):915–936, 2003.
- [45] L. Zdeborová and F. Krzakala. Statistical physics of inference: Thresholds and algorithms. *Advances in Physics*, 65(5):453–552, 2016.